

Magnesite tailing as low-cost adsorbent for the removal of copper (II) ions from aqueous solution

İlker Kıpçak[†] and Turgut Giray Isiyel

Department of Chemical Engineering, Eskişehir Osmangazi University, Eskişehir 26480, Turkey

(Received 1 August 2014 • accepted 17 December 2014)

Abstract—The removal of Cu(II) ions from aqueous solution using magnesite tailing was investigated. Batch kinetic and equilibrium experiments were conducted to study the effects of initial pH, adsorbent dosage, contact time, initial concentration and temperature. The pseudo-first-order, pseudo-second-order and intraparticle diffusion models were used to study the kinetic data. The experimental data were best fitted by the pseudo-second-order kinetic model. The linear Langmuir and Freundlich adsorption equations were applied to describe the equilibrium isotherms. The equilibrium data fit very well the Langmuir model, and the maximum adsorption capacity was estimated as 12.18 mg/g at 45 °C. Thermodynamic parameters such as enthalpy change (ΔH°), free energy change (ΔG°) and entropy change (ΔS°) were calculated, and it was found that the adsorption process was spontaneous and endothermic. The results showed that magnesite tailing is a suitable adsorbent for the removal of Cu(II) ions from aqueous solutions.

Keywords: Adsorption, Cu Removal, Isotherm, Kinetics, Magnesite Tailing

INTRODUCTION

Heavy metal pollution has been observed in industrial wastewaters such as those produced by metal plating facilities, mining operations, battery manufacturing process, the production of paints and pigments, and glass production industry. Intake of heavy metals leads to various health hazards in human beings. Excessive levels of copper leads to mucosal irritation and corrosion, capillary damage, hepatic and renal damage and depression. Gastrointestinal irritation and possible necrotic changes in the liver and kidney could also occur [1]. The permissible limit for Cu(II) in the drinking water approved by WHO is 1 mg L⁻¹ [2]. Minimization and removal of Cu(II) from aqueous systems is therefore an important area of study.

Numerous techniques and treatment technologies have been developed for the clean-up of waters contaminated with copper. Conventional methods employed to remove copper ion from aqueous solutions include chemical precipitation, ion-exchange, membrane filtration, flotation, electrochemical treatment, coagulation, flocculation and adsorption [3]. However, most of these methods have various disadvantages, such as incomplete metal removal, high chemical or energy requirements and formation of toxic sludge, which make these methods incapable or expensive in many cases. Adsorption has been viewed as an effective and simple separation method for the removal of copper. Recent studies have been focused on the development of low-cost, effective and locally available adsorbents for sorption of copper such as natural and activated minerals [4-8], rock samples [9,10], pottery material [11], fly ash [12], sawdust [13], seed shell [14], tree bark [15] and waste biomass [16,

17]. Because of the low cost and high availability of these materials, it is not necessary to have a complicated regeneration process. The literature does not show research about the removal of copper ion using magnesite tailing.

Magnesite is a natural mineral mainly composed of magnesium carbonate. It is widely used as raw material for the production of basic refractories applied in the metallurgical industries. The natural magnesite contains some impurities such as silicon, iron and calcium. In the magnesite plants in Turkey, natural magnesite is generally beneficiated by crushing, screening, scrubbing and magnetic separation. The tailings from these plants still contain a significant amount of usable magnesite, but at a very low grade (MgO equivalent of 35% to 39%). These tailings containing large amounts of impurities are not used anywhere and simply accumulate in the plant areas [18]. It is highly desirable therefore to utilize the magnesite tailings in order to avoid environmental problems.

Thus, the objective of the present study is to explore the effectiveness of using magnesite tailing as a low cost adsorbent for removal of Cu(II) ions from aqueous solutions. The effects of initial pH, adsorbent dosage, contact time, initial concentration and temperature on the removal of Cu(II) were studied. The adsorption kinetics was investigated. Langmuir and Freundlich isotherms were compared with the experimental data. Thermodynamic parameters were also determined.

MATERIALS AND METHODS

1. Materials

The magnesite tailing used in this study was obtained from the KÜMAŞ Plant in Turkey. It was crushed, ground and sieved through a 200 mesh sieve. The sieved tailing sample was dried at 100 °C for 5 hours. The chemical analysis of the magnesite tailing was performed by using X-ray fluorescence analyzer (XRF ARL 8610). The

[†]To whom correspondence should be addressed.

E-mail: ikipcak@ogu.edu.tr

Copyright by The Korean Institute of Chemical Engineers.

chemical composition of the tailing is as follows: 37.80% MgO, 11.17% SiO₂, 6.25% CaO, 0.77% Fe₂O₃, 0.13% Al₂O₃, 0.05% MnO, 0.01% K₂O, 0.01% P₂O₅, <0.01% Na₂O, <0.01% TiO₂ and 43.70% loss on ignition. The X-ray diffractogram of magnesite tailing was obtained using a Philips X'pert Pro diffractometer (XRD) with Cu K α and given in a previous study [19]. The obtained X-ray diffractogram of the tailing showed that it contains magnesite (MgCO₃), quartz (SiO₂) and dolomite (CaMg(CO₃)₂). The BET specific surface areas and average pore diameters of magnesite tailing and Cu(II)-loaded magnesite tailing were determined from N₂ adsorption isotherm with a surface area analyzer (Quantachrome, Autosorb-1 C). Fourier transform infrared spectroscopy (FTIR) spectra of unloaded and Cu(II)-loaded adsorbents were recorded using KBr pellets on a PerkinElmer spectrum 100 Model infrared spectrophotometer over 400–4,000 cm⁻¹. The scanning electron microscopy (SEM) analyses were done in a JSM 5600LV scanning microscope.

The chemicals used during the experiments and analyses were reagent-grade Merck products. A stock solution of 1,000 mg L⁻¹ Cu(II) was prepared by dissolving required amount of CuCl₂·2H₂O in distilled water and was used to prepare the adsorbate solutions by appropriate dilution. The pH value of the solution was adjusted using diluted NaOH and HCl solutions. The pH value was measured by a pH meter (Hanna HI 8314).

2. Methods

Adsorption experiments were performed separately in a batch process. A fixed amount of magnesite tailing and 50 mL of Cu(II) solution were placed in capped volumetric flask and shaken at 150 rpm using a temperature-controlled water bath (Nüve) with shaker (Memmert) for determined time intervals at constant temperatures. After adsorption, the adsorbent was filtered and the Cu(II) concentration retained in the solution was analyzed by atomic absorption spectrophotometer (Thermo ICE 3300) at a wavelength of 324.8 nm. Percentage of Cu(II) removal was then calculated as follows:

$$\text{Removal (\%)} = \frac{C_0 - C_t}{C_0} * 100 \quad (1)$$

where C₀ and C_t are the concentrations in the solution (mg L⁻¹) at time t=0 and at time t (min), respectively. From the mass balance, the amount of copper adsorbed was then calculated to obtain the adsorption capacity by

$$q_t = \frac{(C_0 - C_t) * V}{m} \quad (2)$$

where q_t is the mass of copper adsorbed per unit mass of adsorbent (mg g⁻¹), V is the volume of the treated solution (L) and m is the mass of adsorbent (g).

In the first stage of the adsorption studies, the initial pH of the adsorption medium was changed from 2 to 6 to obtain optimum initial pH value. Then, different adsorbent dosages (0.1–2.0 g/50 mL) were applied to investigate the effect of adsorbent dosage on the adsorption of Cu(II) ions. Batch experiments were also repeated for various time intervals (5–1,440 min) to determine when the adsorption equilibrium was reached for the temperatures of 25, 35 and 45 °C. The initial Cu(II) concentration was varied from 10 to 50 mg L⁻¹ at 25, 35 and 45 °C to determine the effect of initial concentration on the equilibrium uptake of Cu(II).

RESULTS AND DISCUSSION

1. Effect of Initial pH

The pH of an aqueous solution is an important controlling parameter in the process of adsorption. Solution pH affects both aqueous chemistry and surface binding sites of the adsorbent. The dominant species of copper at pH 3.0–5.0 were Cu²⁺ and Cu(OH)⁺, while at pH > 6.3 the species were insoluble Cu(OH)₂ [5,20]. Thus, the experiments were performed in the pH range of 2–6. The effect of pH on the adsorption of Cu(II) ions from aqueous solution by magnesite tailing is illustrated in Fig. 1. It can be observed that the initial pH value greatly influenced the adsorption capacity of magnesite tailing. It increased from 1.15 mg g⁻¹ to 6.54 mg g⁻¹ as the pH increased from 2 to 6. The decrease of the adsorption capacity at lower pH values is apparently due to the higher concentration of H₃O⁺ ions present in the reaction mixture, which compete with the Cu(II)

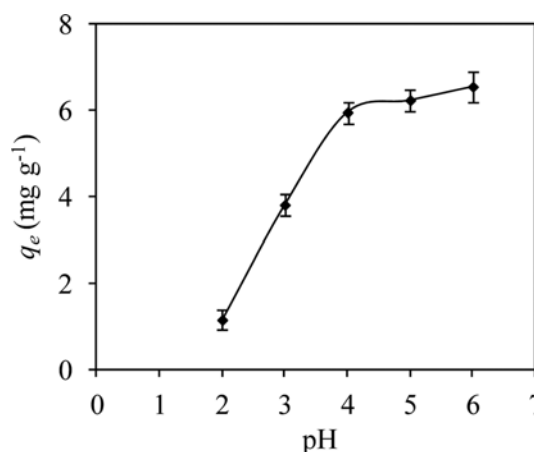


Fig. 1. Effect of initial pH on the adsorption of Cu(II) ions by magnesite tailing (adsorbent dosage=0.1 g/50 mL, contact time=24 h, initial Cu(II) concentration=50 mg L⁻¹, temperature=25 °C, vertical bars represent the standard errors of duplicate determinations).

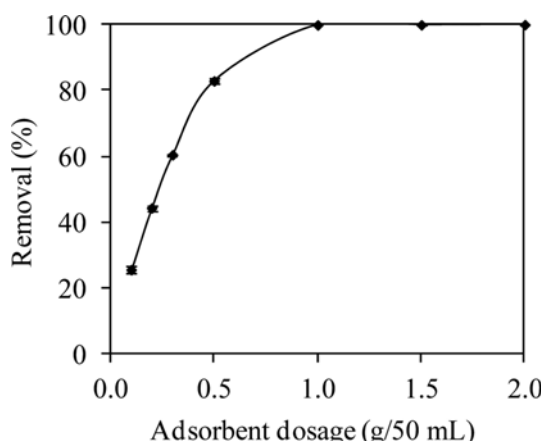


Fig. 2. Effect of adsorbent dosage on the removal of Cu(II) ions by magnesite tailing (pH=6.0, contact time=24 h, initial Cu(II) concentration=50 mg L⁻¹, temperature=25 °C, vertical bars represent the standard errors of duplicate determinations).

ions for the adsorption sites of magnesite tailing. At higher pH values, the concentration of H_3O^+ is smaller, and some of the sites become available to the metal ions resulting in a higher adsorption of Cu(II) ions.

2. Effect of Adsorbent Dosage

Adsorbent dosage is an important parameter because it determines the capacity of an adsorbent for a given initial concentration of the adsorbate at the operating conditions. The study of adsorbent dosage for the removal of the Cu(II) ions from aqueous solution was carried out at different magnesite tailing dosages (0.1-2.0 g/50 mL) using 50 mg L^{-1} of the Cu(II) ion solutions (Fig. 2). The removal of Cu(II) ions increased with increasing adsorbent dosage, and the removal was almost constant at higher dosages than 1.0 g/50 mL. With increasing adsorbent dosage, larger surface area was available for adsorption due to increase in active sites on the adsorbent and thus Cu(II) removal increased. When the adsorbent dosage increased from 0.1 g/50 mL to 2.0 g/50 mL, Cu(II) removal increased from 25.56% to 99.99%.

3. Effect of Contact Time and Temperature

The effect of contact time on the adsorption of Cu(II) ions onto magnesite tailing was studied by using various time intervals (5-1,440 min) at three different temperatures of 25, 35 and 45 °C (Fig. 3). It can be seen that the adsorbent capacity increases with increasing contact time. The initial adsorption rate of Cu(II) ions was very high, as a large number of adsorption sites are available for adsorption at the beginning of the process. The maximum Cu(II) adsorption

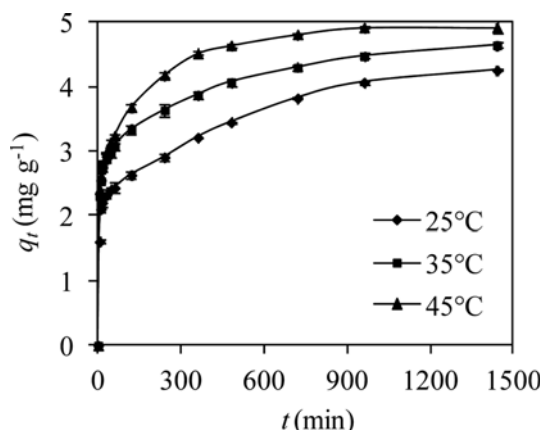


Fig. 3. Effect of contact time on the adsorption of Cu(II) ions by magnesite tailing at different temperatures (pH=6.0, adsorbent dosage=0.5 g/50 mL, initial Cu(II) concentration=50 mg L^{-1} , vertical bars represent the standard errors of duplicate determinations).

(equilibrium) capacity of magnesite tailing was observed at 1,440 min for 25 and 35 °C and 960 min for 45 °C, beyond which there is no further increase in the adsorption capacity. Fig. 3 also shows the effect of the temperature on the adsorption of Cu(II) onto magnesite tailing. The adsorption capacity of magnesite tailing increased with an increase in the temperature from 25 to 45 °C. This situation indicated that the adsorption process was endothermic.

4. Adsorption Kinetics

Kinetics of adsorption is one of the most important characteristics to be responsible for the efficiency of adsorption. Various kinetic models including the pseudo-first-order, pseudo-second-order and intraparticle diffusion have been applied for the experimental data to predict the adsorption kinetics. Among them pseudo-first-order rate equation is given as [21]:

$$\log(q_e - q_t) = \log q_e - k_1 t / 2.303 \quad (3)$$

where q_e and q_t are the respective amounts of Cu(II) adsorbed (mg g^{-1}) at equilibrium and at time t (min), and k_1 is the rate constant of the pseudo-first-order adsorption process (min^{-1}). The slopes and intercepts of plots of $\log(q_e - q_t)$ versus t are used to determine k_1 and q_e values (plots not shown). The pseudo-second-order equation is expressed as [22]:

$$t/q_t = 1/k_2 q_e^2 + t/q_e \quad (4)$$

where k_2 is the rate constant of pseudo-second-order adsorption ($\text{g mg}^{-1} \text{min}^{-1}$). The plot t/q_t versus t should give a straight line if pseudo-second-order kinetics is applicable and q_e and k_2 can be determined from the slope and intercept, respectively (Fig. 4). The

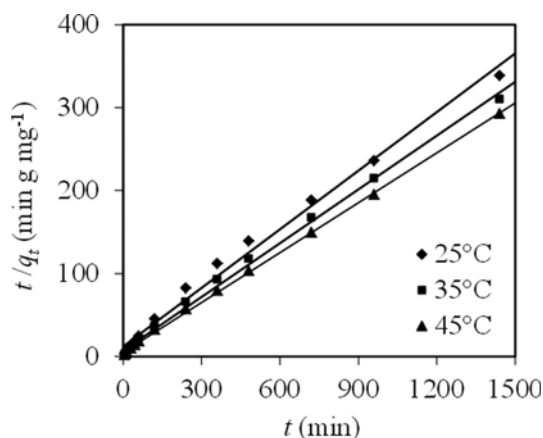


Fig. 4. Pseudo-second-order kinetic plots for the adsorption of Cu(II) ions by magnesite tailing at different temperatures.

Table 1. Kinetic parameters for the adsorption of Cu(II) ions by magnesite tailing at different temperatures

| T (°C) | q_{exp} (mg g^{-1}) | Pseudo-first-order | | | Pseudo-second-order | | | Intraparticle diffusion | | |
|-----------|-------------------------------------|---------------------------------|--------------------------------|-------|---------------------------------|---|-------|---|-----------------------------|-------|
| | | q_e (mg g^{-1}) | k_1 (min^{-1}) | R^2 | q_e (mg g^{-1}) | k_2 ($\text{g mg}^{-1} \text{min}^{-1}$) | R^2 | k_p ($\text{mg g}^{-1} \text{min}^{-1/2}$) | C (mg g^{-1}) | R^2 |
| 25 | 4.25 | 2.26 | 0.003 | 0.982 | 4.24 | 0.005 | 0.991 | 0.069 | 1.854 | 0.968 |
| 35 | 4.64 | 1.96 | 0.003 | 0.989 | 4.63 | 0.007 | 0.997 | 0.064 | 2.507 | 0.953 |
| 45 | 4.92 | 2.24 | 0.004 | 0.994 | 4.99 | 0.008 | 0.999 | 0.076 | 2.625 | 0.895 |

intraparticle diffusion equation can be written as follows [23]:

$$q_t = k_p t^{1/2} + C \quad (5)$$

where k_p is the intraparticle diffusion rate constant ($\text{mg g}^{-1} \text{min}^{-1/2}$) and C is the intercept (mg g^{-1}). According to this model, the plots of q_t versus $t^{1/2}$ (plots not shown) should be linear if intraparticle diffusion is involved in the adsorption system.

The kinetic parameters for the adsorption of Cu(II) onto magnesite tailing are given in Table 1. The pseudo-second-order kinetic model is in good agreement with the experimental data. Its correlation coefficients are higher than those of the pseudo-first-order and the intraparticle diffusion models, and the calculated q_e values agree very well with the experimental ones (q_{exp}). These results imply that the studied adsorption system follows the pseudo-second-order kinetic model at all time intervals.

5. Effect of Initial Concentration

The change in adsorption behavior of magnesite tailing with different Cu(II) ion concentrations ($10\text{--}50 \text{ mg L}^{-1}$) is shown in Fig. 5. The increase in initial Cu(II) ion concentration increased the amount of Cu(II) adsorbed. The initial concentration provided the necessary driving force to overcome the resistances to the mass transfer of adsorbents between the aqueous and solid phases. Therefore, an increase in C_0 enhanced the adsorption of Cu(II) ions. The bigger adsorption capacity was also observed at the higher temperatures.

6. Adsorption Isotherms

The adsorption isotherm is fundamental in understanding the

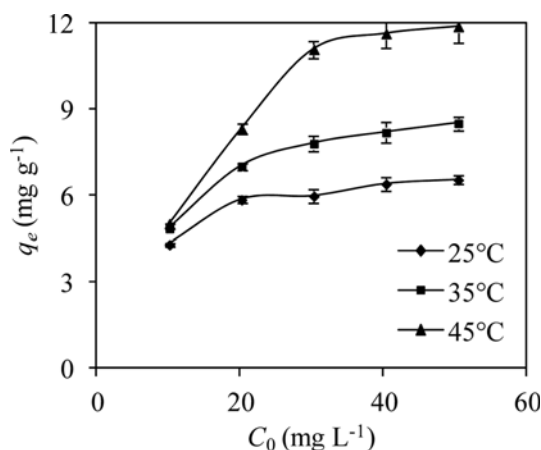


Fig. 5. Effect of initial concentration on the adsorption of Cu(II) ions by magnesite tailing at different temperatures (pH=6.0, adsorbent dosage=0.1 g/50 mL, contact time=24 h, vertical bars represent the standard errors of duplicate determinations).

mechanism of adsorption. Important information regarding how the adsorbate molecules distribute between the liquid phase and the solid phase once the equilibrium state is reached can be interpreted according to the adsorption isotherm. We used the Langmuir and Freundlich isotherm equations to describe the equilibrium of Cu(II) ions adsorption onto magnesite tailing. The Langmuir adsorption isotherm [24] predicts the maximum monolayer adsorption capacity of the adsorbent and also determines if the adsorption is favorable or not. The linearized Langmuir isotherm is represented by following equation:

$$\frac{C_e}{q_e} = \frac{1}{q_0 b} + \frac{C_e}{q_0} \quad (6)$$

where q_e is the adsorbed amount per amount of adsorbent at equilibrium (mg g^{-1}), C_e is the equilibrium concentration in the solution (mg L^{-1}) and the Langmuir constants, q_0 (mg g^{-1}) and b (L mg^{-1}), are the monolayer adsorption capacity and the adsorption equilibrium constant, respectively. To determine if adsorption process is favorable or unfavorable, for the Langmuir type adsorption process, the isotherm can be classified by a term R_L , a dimensionless constant separation factor, which is defined as:

$$R_L = \frac{1}{1 + bC_0} \quad (7)$$

where C_0 is the initial concentration of the adsorbate (mg L^{-1}). The nature of the adsorption process may be either unfavorable ($R_L > 1$), linear ($R_L = 1$), favorable ($0 < R_L < 1$), or irreversible ($R_L = 0$) [25,26]. The Freundlich adsorption isotherm [27] can be applied for non-ideal adsorption on heterogeneous surfaces and multilayer adsorption, and is expressed in linear form by the following equation:

$$\log q_e = \log K_f + \frac{1}{n} \log C_e \quad (8)$$

where K_f (L g^{-1}) and n are Freundlich adsorption isotherm constants, related to the adsorption capacity and the adsorption intensity, respectively.

The various constants of these models were calculated and given in Table 2. By comparing the correlation coefficients, it can be concluded that the Langmuir isotherm provides a good model for the adsorption system, which is based on monolayer adsorption onto surface containing finite number of identical adsorption sites. As shown in Table 2, the calculated values of R_L were found between 0 and 1. This implies that the adsorption of Cu(II) onto magnesite tailing from aqueous solutions is favorable under the conditions used in this study. The maximum adsorption capacities for Cu(II) were observed between 6.69 and 12.18 mg g^{-1} for studied temperatures. The isotherm model fits of the observed equilibrium

Table 2. Langmuir and Freundlich constants for the adsorption of Cu(II) ions by magnesite tailing at different temperatures

| T (°C) | Langmuir | | | Freundlich | | | |
|-----------|------------------------------|----------------------------|-------|-------------|-----------------------------|-------|-------|
| | q_0 (mg g^{-1}) | b (L mg^{-1}) | R^2 | R_L | K_f (L g^{-1}) | n | R^2 |
| 25 | 6.69 | 0.790 | 0.999 | 0.025-0.112 | 4.192 | 7.825 | 0.958 |
| 35 | 8.64 | 0.986 | 0.998 | 0.020-0.092 | 5.525 | 7.955 | 0.998 |
| 45 | 12.18 | 1.263 | 0.997 | 0.016-0.073 | 7.700 | 7.273 | 0.970 |

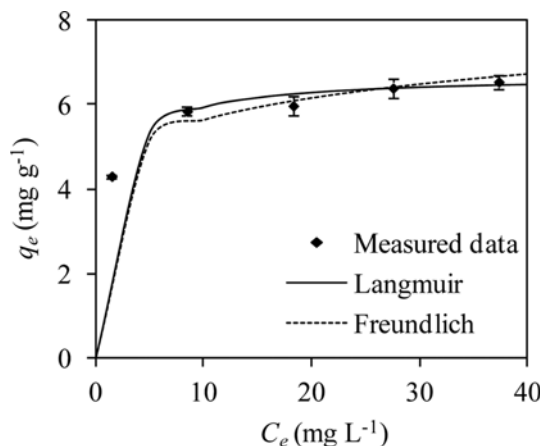


Fig. 6. Isotherm model fits of the observed equilibrium adsorption data of magnesite tailing at 25 °C (vertical bars represent the standard errors of duplicate determinations).

Table 3. Comparisons of the Langmuir adsorption capacities (q_0) for Cu(II) adsorption by different adsorbents

| Type of adsorbent | q_0 (mg g^{-1}) | T (°C) | pH | Refs. |
|---------------------------------|---------------------------------|-----------|-----|---------------|
| Dolomite | 8.3 | 25 | 5.0 | [4] |
| Kaolinite | 9.2 | 30 | 5.7 | [5] |
| Acid-activated kaolinite | 10.1 | 30 | 5.7 | [5] |
| Montmorillonite | 31.8 | 30 | 5.7 | [5] |
| Acid-activated montmorillonite | 32.3 | 30 | 5.7 | [5] |
| Clay containing montmorillonite | 31.0 | - | 2.5 | [6] |
| Bentonite | 44.8 | 23 | 7.0 | [7] |
| Spent activated clay | 13.2 | 27 | 6.0 | [8] |
| Rock sample of scoria | 1.8 | 25 | 5.0 | [9] |
| Phosphate rock | 50.2 | 30 | - | [10] |
| Raw pottery material | 7.6 | 30 | 4.0 | [11] |
| Turkish fly ashes | 1.3 | 20 | 6.0 | [12] |
| Sawdust | 5.4 | 20 | 5.5 | [13] |
| Activated sawdust | 13.5 | 20 | 5.5 | [13] |
| Lentil shells | 9.0 | 20 | 5.0 | [14] |
| Wheat shells | 7.4 | 20 | 6.1 | [14] |
| Rice shells | 1.9 | 20 | 6.0 | [14] |
| Pine bark | 11.9 | 25 | 5.0 | [15] |
| Olive stone | 2.0 | 25 | 5.0 | [15] |
| Areca nut waste | 2.8 | 20 | 5.6 | [16] |
| Tea industry waste | 8.6 | 25 | 5.5 | [17] |
| Magnesite tailing | 6.7 | 25 | 6.0 | Present study |
| Magnesite tailing | 12.2 | 45 | 6.0 | Present study |

adsorption data at 25 °C are shown in Fig. 6. It is obvious that the experimental results are well represented by the Langmuir isotherm.

The maximum adsorption capacities of some adsorbents and magnesite tailing for removal of Cu(II) ions are given in Table 3. The difference of Cu(II) adsorption capacities is due to the properties of each adsorbent such as structure, functional groups and surface area. The experimental data of the present study are com-

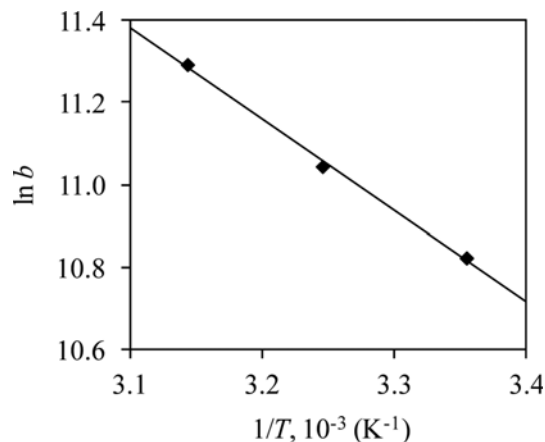


Fig. 7. Plot of $\ln b$ versus $1/T$ for estimation of thermodynamic parameters.

Table 4. Thermodynamic parameters for the adsorption of Cu(II) ions by magnesite tailing

| T (°C) | ΔG° (kJ mol^{-1}) | ΔH° (kJ mol^{-1}) | ΔS° ($\text{J mol}^{-1} \text{K}^{-1}$) |
|--------|---|---|--|
| 25 | -26.83 | | |
| 35 | -28.30 | 18.48 | 151.93 |
| 45 | -29.87 | | |

parable with the reported values.

7. Thermodynamic Parameters

To estimate the effect of temperature on the adsorption of Cu(II) onto magnesite tailing, the free energy change (ΔG°), enthalpy change (ΔH°), and entropy change (ΔS°) were determined. The Langmuir equilibrium constant (b) was used to calculate the thermodynamic parameters using the following equations:

$$\Delta G^\circ = -RT \ln b \quad (9)$$

$$\ln b = \frac{\Delta S^\circ}{R} - \frac{\Delta H^\circ}{RT} \quad (10)$$

where R is the gas constant ($8.314 \text{ J mol}^{-1} \text{ K}^{-1}$) and T is the solution temperature (K). The values of ΔH° and ΔS° were calculated from the slopes and intercepts of the linear regression of $\ln b$ versus $1/T$ (Fig. 7). The calculated parameters are given in Table 4. The negative values of ΔG° (-26.83 , -28.30 and $-29.87 \text{ kJ mol}^{-1}$) confirm the feasibility of the process and the spontaneous nature of the adsorption. The change of free energy for the exchange process is between -8 and -16 kJ mol^{-1} [28]. The ΔG° values up to -20 kJ mol^{-1} show physical adsorption while ΔG° values more negative than -40 kJ mol^{-1} involve chemical adsorption [8]. Therefore, the mechanism of Cu(II) removal by magnesite tailing may be physical adsorption or chemical adsorption. But, the degree of spontaneity increases with temperature. This is because the adsorption process includes principally chemical adsorption rather than physical adsorption. The value of ΔH° ($18.48 \text{ kJ mol}^{-1}$) is positive, indicating that the adsorption reaction is endothermic. The positive value of ΔS° ($151.93 \text{ J mol}^{-1} \text{ K}^{-1}$) indicates a decrease in the order of the system. Thermodynamic data on metal adsorption on natu-

ral minerals agree well with the values obtained in the present work [5,29,30].

8. FTIR Analysis

The FTIR spectra of magnesite tailing and Cu(II)-loaded mag-

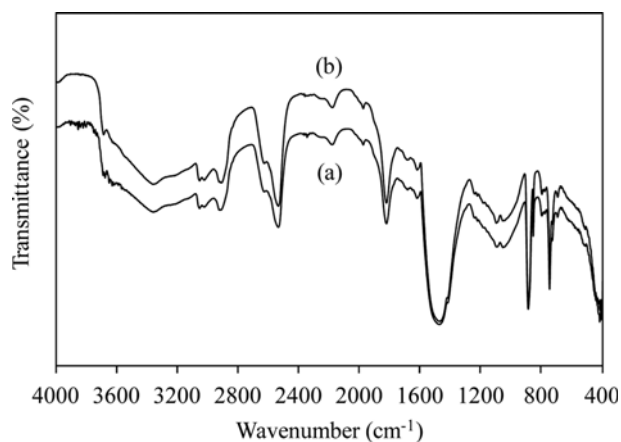


Fig. 8. FTIR spectra of unloaded (a) and Cu(II)-loaded (b) magnesite tailing.

nesite tailing were compared to obtain information on the adsorption of Cu(II) onto the adsorbent (Fig. 8). The possible functional groups for each sample are presented in Table 5. FTIR spectra show that the magnesite tailing mainly composed of carbonate, silicon oxide, iron oxide and hydroxyl groups (Fig. 8(a)) [31]. In the FTIR spectra of unloaded magnesite tailing, the stretching vibrations of the hydroxyl groups were found at the bands ranging from 3,690 to 2,915 cm^{-1} . The adsorption bands at the frequencies of 2,535, 1,825, 1,473 and 1,425 cm^{-1} showed the characteristic stretching of carbonate groups. The weak bands observed at 1,685 and 1,623 cm^{-1} were attributed to the -OH bending [32-35]. The bands at 1,095 and 1,058 cm^{-1} were assigned to the stretching vibration of Si-O-Si group [36,37]. The sharp bands at 890, 858 and 750 cm^{-1} were due to the CO_3^{2-} bending [34,38]. The bands at 800 and 780 cm^{-1} were characteristic of quartz mineral [32]. The band observed at 698 cm^{-1} was produced by Mg-OH bending vibration. The adsorption bands at 420 and 410 cm^{-1} frequencies indicated the presence of Si-O or Fe-O bending vibrations [37,39] (Fig. 8(a)). These groups are likely to be responsible for Cu(II) adsorption. Some peaks (3,678, 3,650, 3,630 and 3,615 cm^{-1}) indicating surface hydroxyl groups disappeared in the FTIR spectra of Cu(II)-loaded magnesite tailing. There were shifts in the -OH stretching bands (from

Table 5. Functional groups in unloaded and Cu(II)-loaded adsorbents

| Functional group | Wavenumber (cm^{-1}) | |
|--|---------------------------------|-------------------------|
| | Unloaded adsorbent | Cu(II)-loaded adsorbent |
| Surface hydroxyl groups (Si-OH-Si) | 3690-3678-3650-3630-3615 | 3688 |
| -OH stretching | 3358-3055-3020-2915 | 3363-3055-3025-2913 |
| CO_3^{2-} stretching-bending | 2535 | 2538 |
| CO_3^{2-} stretching | 1825 | 1825 |
| -OH bending | 1685-1623 | 1688-1620 |
| CO_3^{2-} asymmetric stretching | 1473-1425 | 1473-1420 |
| Si-O stretching vibration | 1095-1058 | 1100-1060 |
| CO_3^{2-} out of plane bending | 890-858 | 890-858 |
| Si-O stretching vibration | 800-780 | 800-783 |
| CO_3^{2-} in plane bending | 750 | 750 |
| Mg-OH bending vibration | 698 | 695 |
| Si-O or Fe-O vibrations | 420-410 | 430-418-408 |

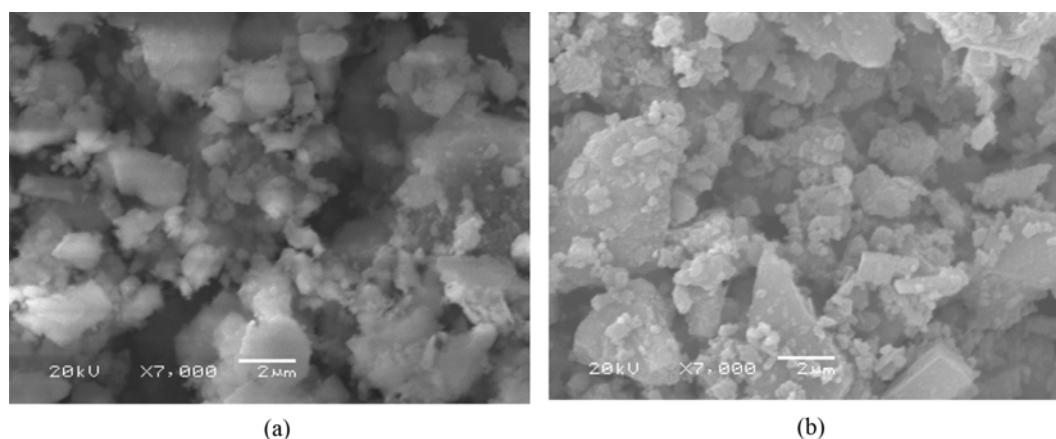


Fig. 9. SEM micrographs of magnesite tailing before (a) and after (b) Cu(II) adsorption.

3,358 to 3,363 cm^{-1} , from 3,020 to 3,025 cm^{-1} and from 2,915 to 2,913 cm^{-1}). Similarly, shifts in the -OH bending (from 1,685 to 1,688 cm^{-1} and from 1,623 to 1,620 cm^{-1}) clearly indicated the involvement of the OH groups as an active site for binding of positively charged copper cations. The shifts in the CO_3^{2-} stretching (from 2,535 to 2,538 cm^{-1} and from 1,425 to 1,420 cm^{-1}), Si-O stretching (from 1,095 to 1,100 cm^{-1} , from 1,058 to 1,060 cm^{-1} and 780 to 783 cm^{-1}) and Mg-OH bending (from 698 to 695 cm^{-1}) vibrations were also observed. The peaks of Si-O or Fe-O bending vibrations at 420 and 410 cm^{-1} were separated into 430, 418 and 408 cm^{-1} peaks (Fig. 8(b)). These shifts in the absorption bands showed the use of hydroxyl, carbonate, silicon oxide and iron oxide groups in the adsorption of copper ions from solution.

9. SEM and BET Analyses

SEM micrographs of magnesite tailing were taken before and after Cu(II) adsorption (Fig. 9). It is clearly observed in Fig. 9 that the surface morphology of Cu(II)-adsorbed magnesite tailing is different from that of natural magnesite tailing. The SEM image of the magnesite tailing revealed its complex and porous surface texture (Fig. 9(a)). After adsorption, large amounts of pores on magnesite tailing disappeared and its surface was covered with many small fragments (Fig. 9(b)). Besides, the average pore diameter of magnesite tailing increased from 9.26 nm to 10.12 nm and the BET surface area decreased from 23.12 m^2g^{-1} to 22.59 m^2g^{-1} after copper adsorption. Some pores may have been occupied by copper ions. The increase of the average pore diameter was due to the reduction of microporous contribution [40]. These results show that the surface morphology of the magnesite tailing changed significantly during the adsorption process. This indicates an important interaction at the Cu-particle interface.

CONCLUSION

The kinetics and equilibrium of the adsorption of Cu(II) from aqueous solution using magnesite tailing were investigated using a batch system. The results indicated that the adsorption capacity of the adsorbent was affected by initial pH, adsorbent dosage, contact time, initial concentration and temperature. The kinetic studies indicated that the experimental data followed the pseudo-second-order kinetic model. The Langmuir isotherm model provided the best fit for the experimental adsorption data, revealing the maximum adsorption capacity for Cu(II) of 12.18 mg per gram of magnesite tailing at 45 °C. The thermodynamic studies showed the spontaneous, endothermic and random nature of the process. The copper-magnesite tailing interactions were confirmed by BET, FTIR and SEM analyses. The hydroxyl, carbonate, silicon oxide and iron oxide groups on the adsorbent surface were found as responsible for Cu(II) adsorption. It may be concluded that the magnesite tailing can be used as a low-cost, natural and abundant source for the removal of Cu(II) ions, and it may be an alternative to more costly materials.

ACKNOWLEDGEMENT

This study was financially supported by Eskişehir Osmangazi University Research Foundation (Project No. 200815036).

REFERENCES

1. M. Ajmal, A. H. Khan, S. Ahmad and A. Ahmad, *Water Res.*, **32**, 3085 (1998).
2. WHO, *Guidelines for Drinking Water Quality, Vol. 1. Recommendations*, World Health Organization, Geneva (1984).
3. M. Bilal, J. A. Shah, T. Ashfaq, S. M. H. Gardazi, A. A. Tahir, A. Pervez, H. Haroon and Q. Mahmood, *J. Hazard. Mater.*, **263**, 322 (2013).
4. E. Pehlivan, A. M. Özkan, S. Dinç and Ş. Parlayıcı, *J. Hazard. Mater.*, **167**, 1044 (2009).
5. K. G. Bhattacharyya and S. S. Gupta, *Desalination*, **272**, 66 (2011).
6. J. U. K. Oubagaranadin and Z. V. P. Murthy, *Appl. Clay Sci.*, **50**, 409 (2010).
7. S. Veli and B. Alyüz, *J. Hazard. Mater.*, **149**, 226 (2007).
8. C.-H. Weng, C.-Z. Tsai, S.-H. Chu and Y. C. Sharma, *Sep. Purif. Technol.*, **54**, 187 (2007).
9. J.-S. Kwon, S.-T. Yun, J.-H. Lee, S.-O. Kim and H. Y. Jo, *J. Hazard. Mater.*, **174**, 307 (2010).
10. M. Prasad, H.-Y. Xub and S. Saxena, *J. Hazard. Mater.*, **154**, 221 (2008).
11. O. Khazali, R. Abu-El-Halawa and K. Al-Souöd, *J. Hazard. Mater.*, **B139**, 67 (2007).
12. B. Bayat, *J. Hazard. Mater.*, **B95**, 251 (2002).
13. F. N. Acar and Z. Eren, *J. Hazard. Mater.*, **B137**, 909 (2006).
14. H. Aydın, Y. Bulut and Ç. Yerlikaya, *J. Environ. Manage.*, **87**, 37 (2008).
15. G. Blazquez, M. A. Martin-Lara, E. Dionisio-Ruiz, G. Tenorio and M. Calero, *J. Ind. Eng. Chem.*, **17**, 824 (2011).
16. W. Zheng, X.-M. Li, F. Wang, Q. Yang, P. Deng and G.-M. Zeng, *J. Hazard. Mater.*, **157**, 490 (2008).
17. S. Çay, A. Uyanık and A. Özaşık, *Sep. Purif. Technol.*, **38**, 273 (2004).
18. M. Özdemir, D. Çakır and İ. Kıpçak, *Int. J. Miner. Process.*, **93**, 209 (2009).
19. İ. Kıpçak and M. Özdemir, *Chem. Eng. J.*, **189-190**, 68 (2012).
20. H. A. Elliott and C. P. Huang, *Water Res.*, **15**, 849 (1981).
21. S. Lagergren, *Handlingar*, **24**, 1 (1898).
22. Y. S. Ho and G. McKay, *Chem. Eng. J.*, **70**, 115 (1998).
23. W. J. Weber and J. C. Morris, *J. Sanitary Eng. Div. ASCE*, **89**, 31 (1963).
24. I. Langmuir, *J. Am. Chem. Soc.*, **40**, 1361 (1918).
25. T. W. Weber and R. K. Chakravorti, *J. Am. Inst. Chem. Eng.*, **20**, 228 (1974).
26. K. R. Hall, L. C. Eagleton, A. Acrivos and T. Vermeulen, *Ind. Eng. Chem. Fund.*, **5**, 212 (1966).
27. H. Freundlich, *Colloid and Capillary Chemistry*, Methuen, London (1926).
28. F. Helfferich, *Ion Exchange*, McGraw-Hill, New York (1962).
29. B. I. Olu-Owolabi and E. I. Unuabonah, *J. Hazard. Mater.*, **184**, 731 (2010).
30. K. G. Bhattacharyya and S. S. Gupta, *Chem. Eng. J.*, **136**, 1 (2008).
31. R. L. Frost and S. Bahfenne, *J. Raman Spectrosc.*, **40**, 360 (2009).
32. A. Sdiri, T. Higashi, T. Hatta, F. Jamoussi and N. Tase, *Chem. Eng. J.*, **172**, 37 (2011).
33. T. B. Musso, M. E. Parolo, G. Pettinari and F. M. Francisca, *J. Environ. Manage.*, **146**, 50 (2014).

34. T. Montanaria, L. Castoldi, L. Lietti and G. Busca, *Appl. Catal. A: Gen.*, **400**, 61 (2011).
35. F. A. Dawodu and K. G. Akpomie, *J Mater. Res. Technol.*, **3**, 129 (2014).
36. T. S. Anirudhan, S. Jalajamony and S. S. Sreekumari, *Appl. Clay Sci.*, **65-66**, 67 (2012).
37. W. Ma, X. Song, Y. Pan, Z. Cheng, G. Xin, B. Wang and X. Wang, *Chem. Eng. J.*, **193-194**, 381 (2012).
38. Y. S. Al-Degs, M. I. El-Barghouthi, A. A. Issa, M. A. Khraisheh and G. M. Walker, *Water Res.*, **40**, 2645 (2006).
39. T. S. Anirudhan and P. S. Suchithra, *Chem. Eng. J.*, **156**, 146 (2010).
40. C. H. Lai, S. L. Lo and H. L. Chiang, *Chemosphere*, **41**, 1249 (2000).